Supporting Information

β-Carotene Probes the Energy Transfer Pathway in the Photosystem II Core Complex.

Yusuke Yoneda[1], Yutaka Nagasawa[2], Yasufumi Umena[3], Hiroshi Miyasaka[1]

[1]*Graduate School of Engineering Science, Osaka University, Toyonaka Osaka 560-8531, Japan*

[2]*College of Life Science, Ritsumeikan University, Kusatsu, Shiga 525-8577, Japan*

[3]*Research Institute for Interdisciplinary Science, Okayama University, Okayama, Okayama 700-8530 Japan*

Table of Contents page

Materials and Methods

Preparation of PSII-CC. Dimeric PSII-CC was separated and purified from the thermophilic cyanobacterium *Thermosynechococcus vulcanus* as described previously[1,2] in a 30 mM 2-(N-morpholino)-ethanesulfonic acid (MES) buffer, containing 20 mM NaCl, 3 mM $CaCl_2$, 0.03%w/v n-Dodecyl beta-D-maltoside, 5%w/v glycerol. Dimeric PSII-CC was further improved its quality by re-crystallization steps.[1,3,4] Then the dimeric PSII-CC crystals were transferred into the buffer solution and used for TA spectroscopy measurement.

Transient absorption spectroscopy. The experimental set up for TA measurements is similar to those utilized in previous studies.[5,6] The femtosecond Ti:Sapphire laser (Tsunami, Spectra-Physics) was pumped by the SHG of a cw Nd^{3+}:YVO_4 laser (Millennia V, Spectra-Physics). The output of Ti:Sapphire laser was regeneratively amplified with 1 kHz repetition rate (Spitfire, Spectra-Physics) and the amplified pulse had an energy of 1 mJ / pulse and pulse duration of 85 fs fwhm. The amplified pulse was divided into two pulses with a 50/50% beam splitter and guided into a pair of collinear optical parametric amplifier systems (TOPAS-Prime, Light-Conversion). The wavelength of the outputs of TOPAS-Prime were controlled by computers. The polarization between the pump and probe pulses was set at magic angle. The optical path of the sample cell was 1 mm, and the optical density of the

sample was ~0.8 at 676 nm. A homemade rotating cell was used (2000 rpm) to avoid optical damage of the sample and accumulation of long-lived species. The distance from the center of the rotating cell to the laser focusing point was ~5 mm, thus, the length of periphery is ~31 mm and the rotation velocity is ~1.0 m/sec. Assuming a focused spot size of ~0.3 mm, it requires ~100 shots before hitting the same position. Moreover, the PSII-CC particle could diffuse, because the sample is a solution. The fluctuation of the individual laser pulse was observed by oscilloscope, and was estimated to be less than 10 %.

The output of TOPAS-Prime with its spectrum centered at 510 nm and 490 nm (fwhm width ~ 5 nm) were utilized to excite the PSII-CC. Meanwhile, by focusing the output of the other TOPAS-Prime (center wavelength: 1180 nm) into a rotating CaF_2 window (optical path: 2 mm), white-light supercontinuum was generated. The instrument response time was estimated to be 45 fs by data analysis. The signal and the reference pulses in the wavelength range of 410-950 nm were detected with two pairs of spectrometer and multichannel photodiode array system (PMA-10, Hamamatsu) and the data were sent to a personal computer for further analysis.

The time dependence of transient absorbance at various wavelength was simultaneously analyzed by global fitting using Glotaran software based on R package

TIMP.[7,8] A sequential model with increasing lifetimes with 100 % yield was used to reproduce the signal where each spectrum evolves into the next one with each lifetime. These evolution associated difference spectra (EADS) are not necessarily corresponds to “pure states” and are used to describe the time evolution of the data.

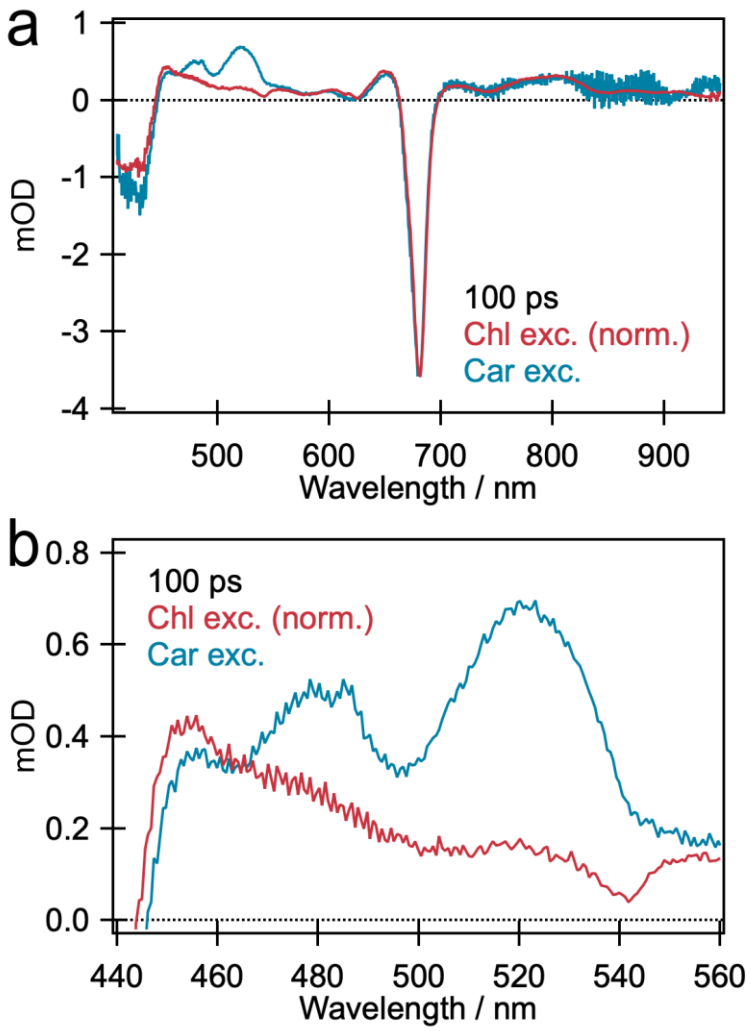

Figure S1. Transient absorption spectra of PSII-CC excited at 640 nm (chlorophyll excitation; red) and 490 nm (β-carotene excitation; blue) in the wavelength range of (a) 410-950 nm and (b) 440-560 nm.

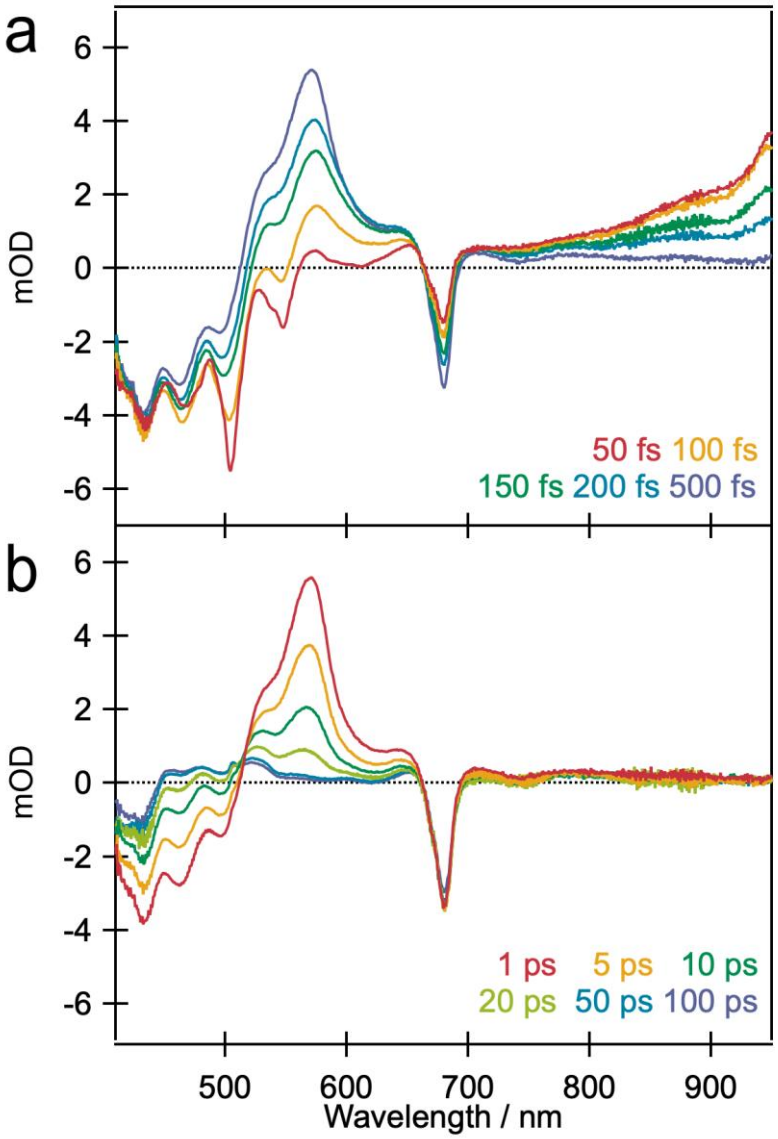

Figure S2. Transient absorption spectra of photosystem II core complex excited at 510 nm in time range of (a) 50 - 500 fs and (b) 1 - 100 ps.

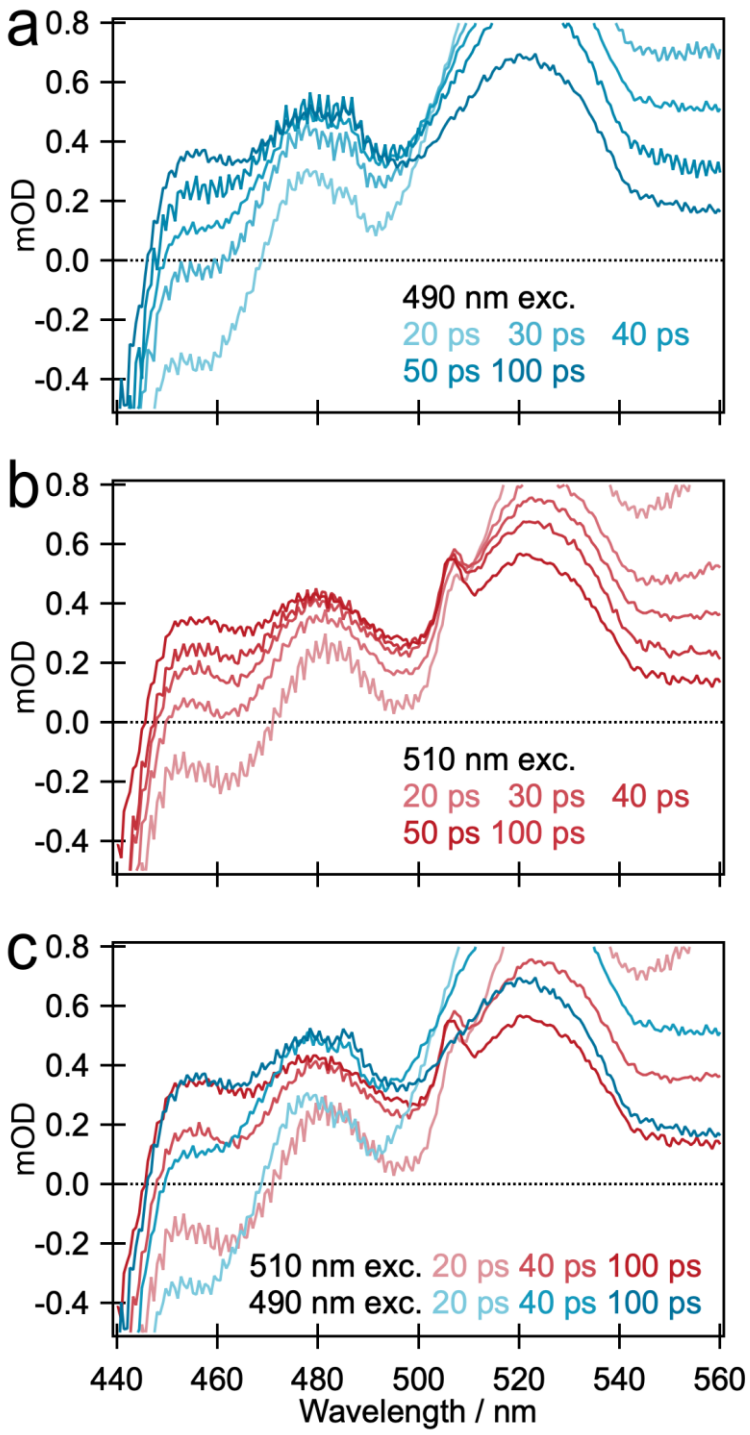

Figure S3. Transient absorption spectra of PSII-CC excited at (a) 490 nm and (b) 510 nm. (c) Comparison between transient absorption spectra of PSII-CC excited at 490 nm and 510 nm.

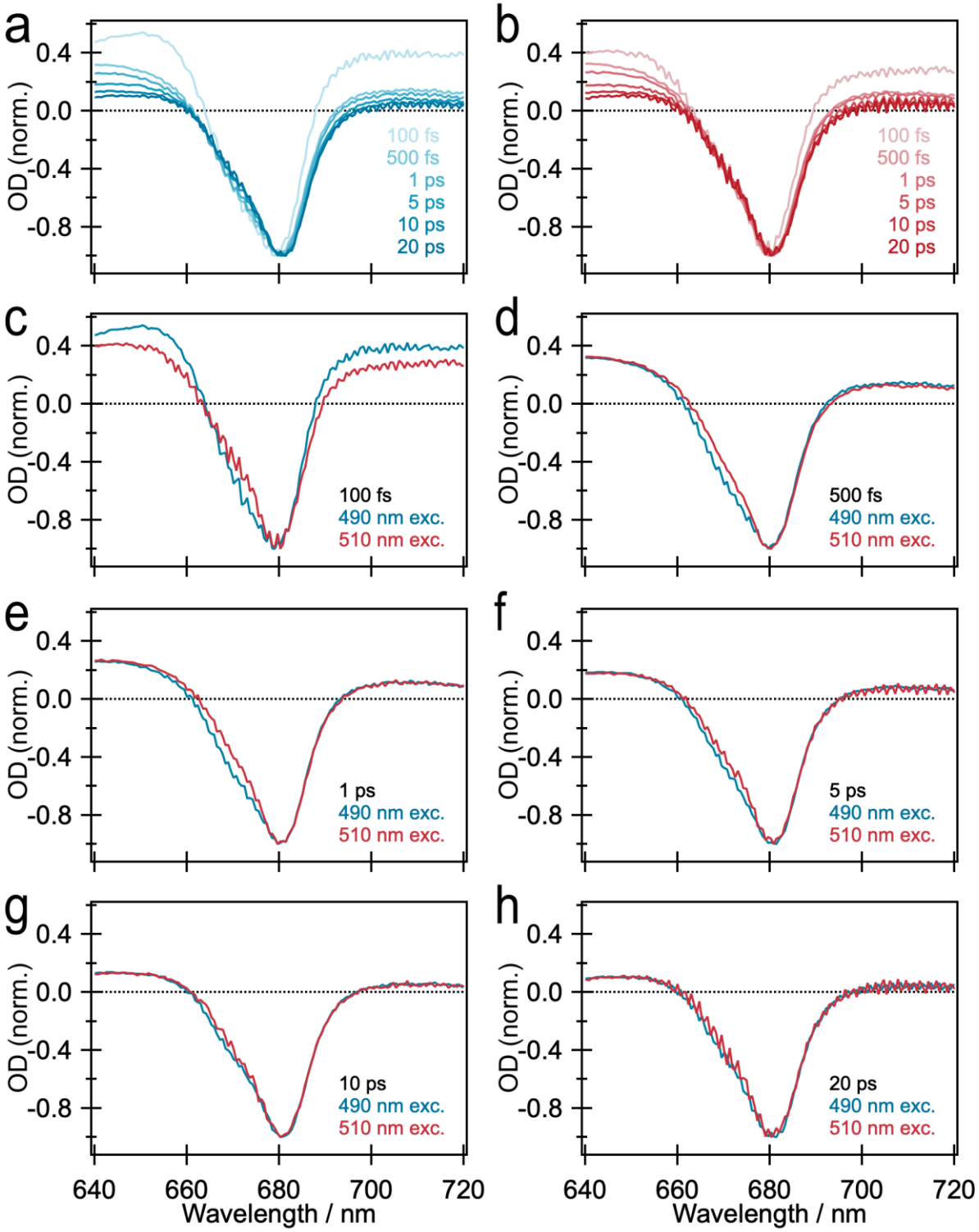

Figure S4. Transient absorption spectra of PSII-CC excited at (a) 490 nm and (b) 510 nm. Comparison between transient absorption spectra of PSII-CC excited at 490 nm and 510 nm at (c) 100 fs, (d) 500 fs, (e) 1 ps, (f) 5 ps, (g) 10 ps and (h) 20 ps.

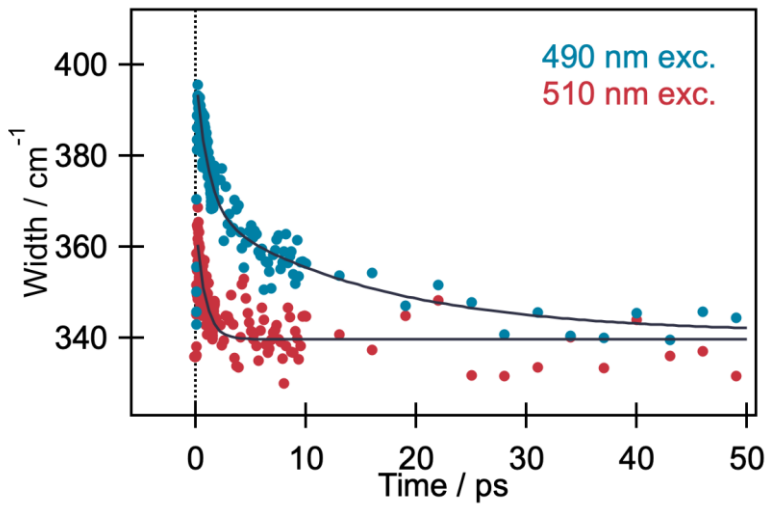

Figure S5. Time evolution of the width of the ground state bleach of chlorophyll at 680 nm. The signals were reproduced by exponential functions with time constants of 1.1 and 16 ps for 490 nm excitation, and 0.82 ps for 510 nm excitation.

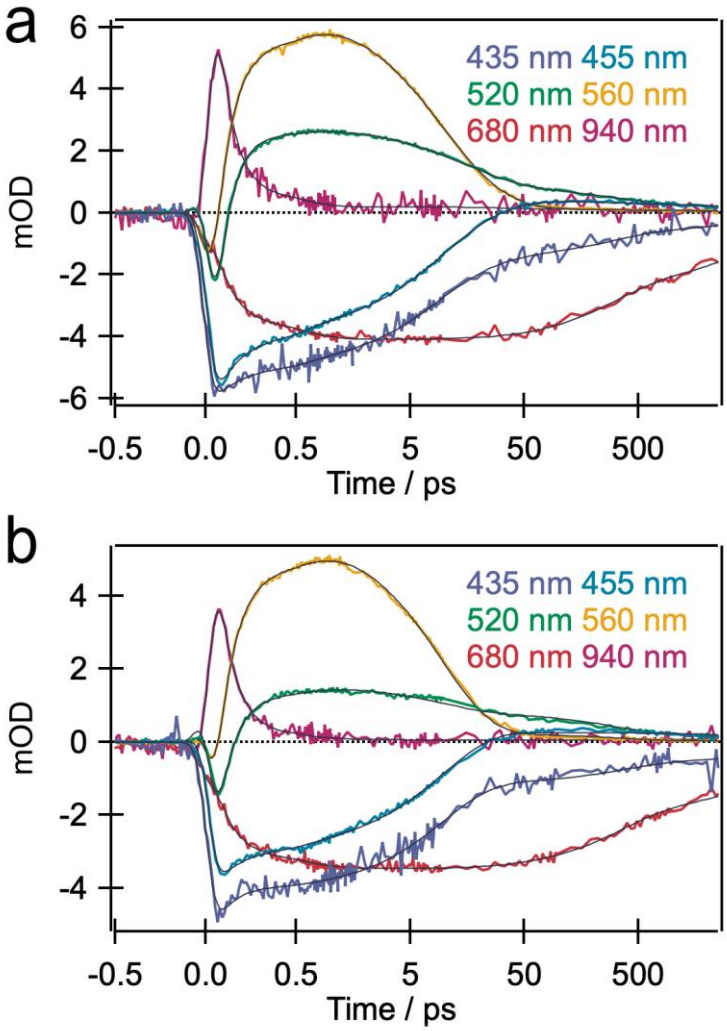

Figure S6. Time traces of transient absorbance of PSII-CC at various probe wavelength excited at (a) 490 nm and (b) 510 nm. Black curves show the result of global fitting. The time axis is linear at -0.5 to 0.5 ps and logarithmic at later delay time.

Inspection of the Number of Components in Global Fitting

To confirm the adequacy of number of components in global fitting, singular value decomposition was performed to transient absorption dataset of PSII-CC.

In the case of 490 nm excitation, as can be seen from Figure S7a, there seems to be at least 5 components and perhaps 6. In this case, the structure of the left and right singular vectors should be taken into account. Left and right singular vectors represent time dependence of the particular components and spectral dependence of the particular components. In this case, the 6th component still shows significant structure of the left and right vectors distinct from noise. And thus, 6 components should be adequate to analyze the transient absorption data of 490 nm excitation.

On the other hand, in the case of 510 nm excitation, as can be seen from the singular values (Figure S8a), first 5 components are significantly different from the rest. Thus, 5 components should be enough for a good fitting in global analysis.

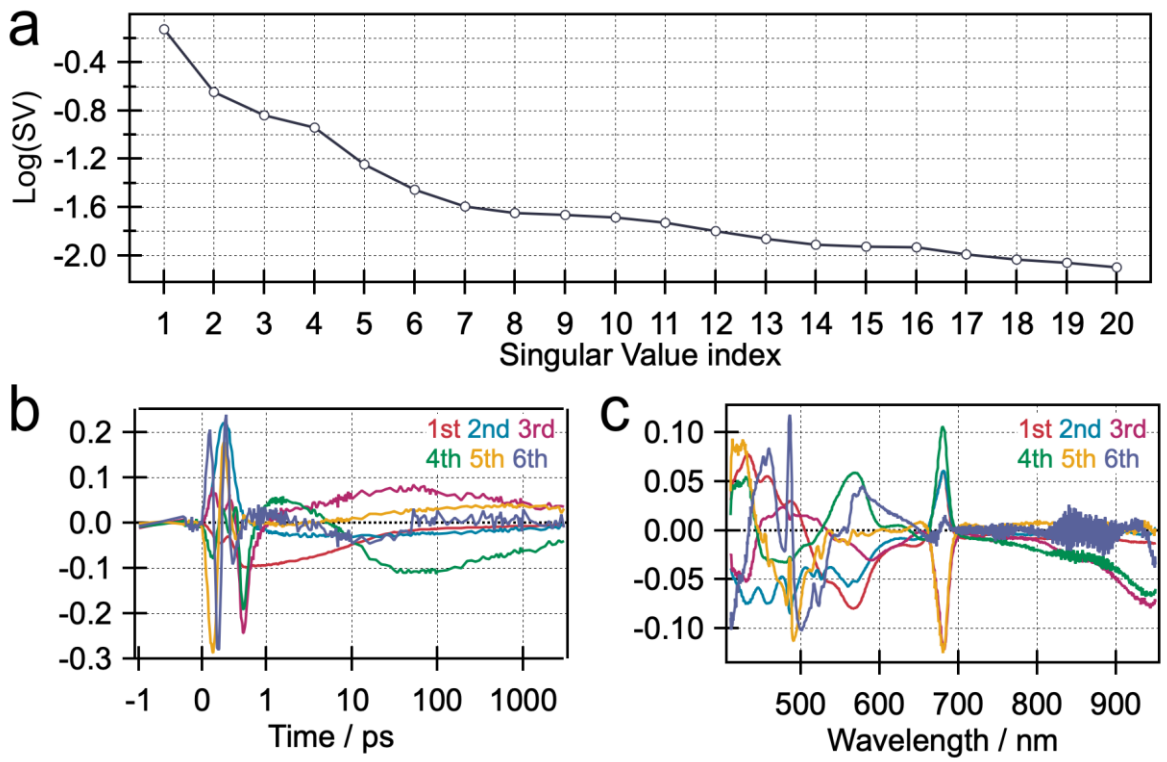

Figure S7. The singular value decomposition of the transient absorption spectra of PSII-CC excited at 490 nm. (a) The first 20 singular values. (b) The first 6 left singular vectors. The time axis is linear at -1 to 1 ps and logarithmic at later delay time. (c) The first 6 right singular vectors.

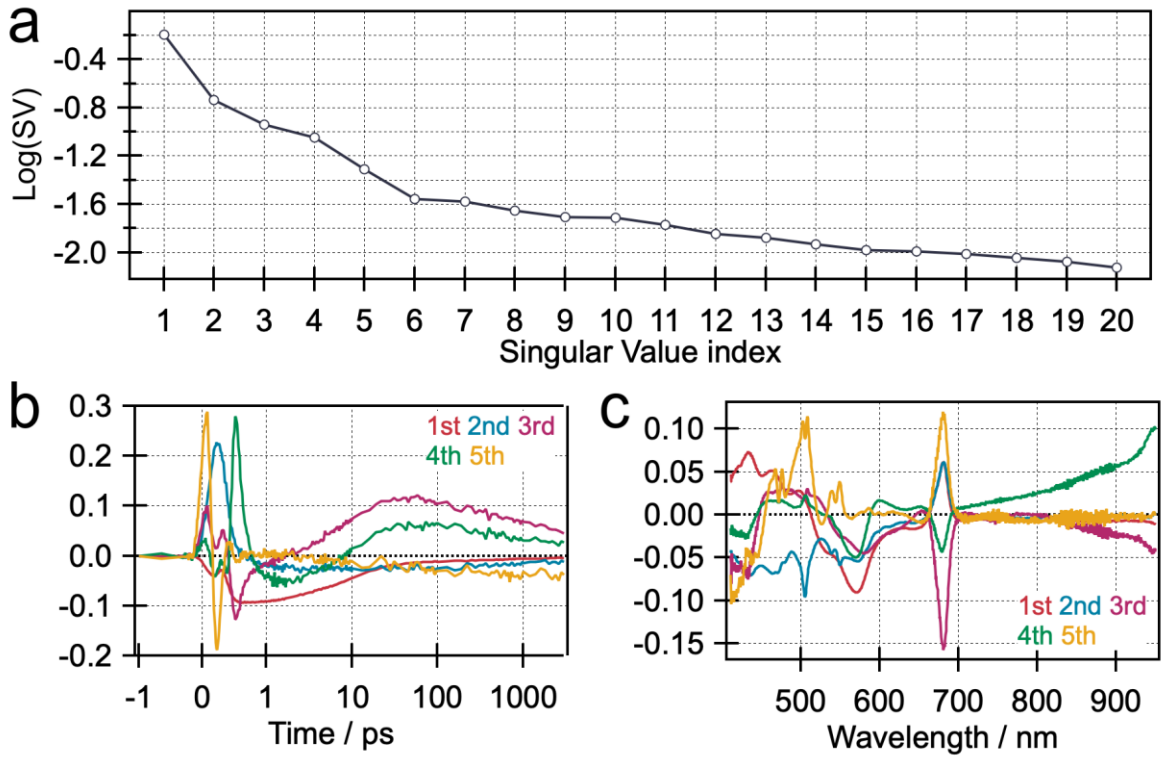

Figure S8. The singular value decomposition of the transient absorption spectra of PSII-CC excited at 510 nm. (a) The first 20 singular values. (b) The first 5 left singular vectors. The time axis is linear at -1 to 1 ps and logarithmic at later delay time. (c) The first 5 right singular vectors.

Detailed Discussion of EADS

In the case of 510 nm excitation (Fig. 4a), the contribution from the charge separated (CS) state seems to appear when the GSB of Bcr disappears, *i.e.*, the negative signal below 500 nm which is present in the 3rd EADS is absent in the 4th. However, it is quite apparent that energy transfer (ET) from the S_1 state of Bcr is negligible, because deepening of the GSB of chlorophyll (Chl) is only observable between the first and second EADS. Thus, CS state should be formed by the ET from the S_2 state of Bcr.

For 490 nm excitation (Figure 4b), one may assume that the 4th EADS with time constant of 20 ps is due to vibrationally hot ground state of Bcr. Lenzer *et al*. reported that vibrationally hot ground state of Bcr in *n*-hexane appears and disappears with time constants of 8.7 ps and 11.9 ps,[9] which are comparable to those of the 3rd and the 4th EADS. Most prominent hot band is expected to appear in the range of 520-550 nm, at the red edge of the S_0 absorption,[9] which should be overlapped with the $T_1 \rightarrow T_n$ transition band of Bcr.[10] However, the width of the Chl GSB at 680 nm is narrower for the 5th EADS than that of the 4th, indicating that ET is taking place simultaneously with cooling of the hot ground state. Time evolution of the bandwidth of the Chl GSB (Fig. S5) also supports this conclusion. If the band at 455 nm appears simultaneously with the hot ground state, it should be easily detected in the

4th EADS because the intensities of the 4th and the 5th EADS are comparable. Thus, we conclude that CS takes place with time constant of ~20 ps following the ET to the reaction center.

It is also worth mentioning that the ET efficiency from the S_2 state of Bcr to Chl can be roughly estimated by EADS although current sequential modeling assumes 100 % yield for each step. The yield can be estimated from the integrated ratio between GSB of Bcr in the 1st and the 2nd EADS by assuming that there are only two relaxation pathways from the S_2 state; internal conversion (Bcr $S_2 \rightarrow S_1$) and ET (Bcr $S_2 \rightarrow$Chl). There are many other contributions in EADS such as excited state absorption of Bcr or Chl and *etc.*, thus, GSB signal was integrated at 410-450 nm to minimize unwanted contributions. The estimated yield of the ET was ~0.3 for both excitation wavelengths, which is comparable to the value of 0.35 obtained by fluorescence excitation spectrum.[11] After the ET to Chl, the yields for sequential steps should be the same as those for Chl excitation. No evidence was obtained which indicates that the yields of ET and CS are significantly different for 510 and 490 nm excitation.

Table S1. Time constants and standard errors obtained by global analysis (in ps unit).

	510 nm excitation	490 nm excitation
1st	0.085 ± 0.000	0.074 ± 0.000
2nd	0.43 ± 0.00	0.36 ± 0.00
3rd	9.6 ± 0.0	7.4 ± 0.1
4th	340 ± 0	20 ± 0
5th	> 2000	290 ± 10
6th	-	> 2000

References

(1) Shen, J. R.; Kamiya, N. Crystallization and the Crystal Properties of the Oxygen-Evolving Photosystem II from Synechococcus Vulcanus. *Biochemistry* **2000**, *39*, 14739–14744.

(2) Shen, J. R.; Inoue, Y. Binding and Functional Properties of Two New Extrinsic Components, Cytochrome c-550 and a 12-KDa Protein, in Cyanobacterial Photosystem II. *Biochemistry* **1993**, *32*, 1825–1832.

(3) Umena, Y.; Kawakami, K.; Shen, J. R.; Kamiya, N. Crystal Structure of Oxygen-Evolving Photosystem II at a Resolution of 1.9Å. *Nature* **2011**, *473*, 55–60.

(4) Kamiya, N.; Shen, J.-R. Crystal Structure of Oxygen-Evolving Photosystem II from Thermosynechococcus Vulcanus at 3.7-A Resolution. *Proc. Natl. Acad. Sci.* **2003**, *100*, 98–103.

(5) Yoneda, Y.; Noji, T.; Katayama, T.; Mizutani, N.; Komori, D.; Nango, M.; Miyasaka, H.; Itoh, S.; Nagasawa, Y.; Dewa, T. Extension of Light-Harvesting Ability of Photosynthetic Light-Harvesting Complex 2 (LH2) through Ultrafast Energy Transfer from Covalently Attached Artificial Chromophores. *J. Am. Chem. Soc.* **2015**, *137*, 13121–13129.

(6) Yoneda, Y.; Katayama, T.; Nagasawa, Y.; Miyasaka, H.; Umena, Y. Dynamics of Excitation Energy Transfer Between the Subunits of Photosystem II Dimer. *J. Am. Chem. Soc.* **2016**, *138*, 11599–11605.

(7) Snellenburg, J. J.; Laptenok, S. P.; Seger, R.; Mullen, K. M.; van Stokkum, I. H. M. Glotaran : A Java -Based Graphical User Interface for the R Package TIMP. *J. Stat. Softw.* **2012**, *49*.

(8) Mullen, K. M.; Stokkum, I. H. M. van. TIMP : An R Package for Modeling Multi-Way Spectroscopic Measurements. *J. Stat. Softw.* **2007**, *18*, 1–7.

(9) Lenzer, T.; Ehlers, F.; Scholz, M.; Oswald, R.; Oum, K. Assignment of Carotene S* State Features to the Vibrationally Hot Ground Electronic State. *Phys. Chem. Chem. Phys.* **2010**, *12*, 8832–8839.

(10) Mathis, P. Etude par Spectroscopie D'eclairs du Transfert D'energie Chlorophylle -Carotenoide. *Photochem. Photobiol.* **1969**, *9*, 55–63.

(11) de Weerd, F. L.; Dekker, J. P.; van Grondelle, R. Dynamics of Beta-Carotene-to-Chlorophyll Singlet Energy Transfer in the Core of Photosystem II. *J. Phys. Chem. B* **2003**, *107*, 6214–6220.